Solute–Solvent Interactions of Glycine, L-Alanine and L-Valine in Aqueous $ZnCl_2$ and $CuCl_2$ Media: A Volumetric, Viscometric and Acoustic Study

Prof. Kalpana Shahi[1*], Dr. Brameshwar[2], DPrashant Kumar[3]

[1] Department of Chemistry, College of Commerce, Arts and Science, Patna, Bihar, India
E-mail: drkalpanashahi@gmail.com
[2]Department of Chemistry, A.N. College, Patna, Bihar, India
E-mail: drbrameshwar254@gmail.com
[3]Research Scholar, Department of Chemistry, Patliputra University, Patna, Bihar, India
E-mail: dprashant.bunty@gmail.com

Abstract:
The thermodynamic and transport properties of three biologically significant α-amino acids — glycine, L-alanine and L-valine — were systematically investigated in aqueous zinc chloride ($ZnCl_2$) and copper(II) chloride ($CuCl_2$) solutions over the temperature range 298.15–318.15 K. Apparent molar volumes (V_φ), Jones–Dole viscosity B-coefficients, and isentropic compressibilities (κ_S) were determined from precise density, viscosity and ultrasonic speed measurements as functions of amino acid concentration (0.05–0.50 mol L^{-1}) and salt molality (0.1–2.0 mol kg^{-1}). Limiting apparent molar volumes (V_φ°) were extracted via the Masson equation, and transfer volumes ($\Delta_t V_\varphi^\circ$) were computed by referencing V_φ° values in pure water. The viscosity data were rationalized through the Jones–Dole formalism to yield A and B coefficients, with the B-coefficient serving as a quantitative marker of ion–solvent interactions. Fourier-transform infrared (FTIR) spectra unambiguously confirmed inner-sphere coordination of Cu^{2+} through a bathochromic shift of the asymmetric COO^- stretching vibration ($\Delta\nu = -23$ to -25 cm^{-1}), diagnostic of bidentate N,O-chelation, whereas Zn^{2+} produced a smaller shift ($\Delta\nu = -11$ to -14 cm^{-1}) consistent with predominantly monodentate oxygen coordination. Transfer volumes for both $ZnCl_2$ and $CuCl_2$ media were substantially larger than the corresponding values previously reported for alkaline-earth chlorides ($MgCl_2$, $CaCl_2$), demonstrating the dominant role of partial covalent/chelate character in d-block cation–amino acid interactions. The order $\Delta_t V_\varphi^\circ(Cu^{2+}) > \Delta_t V_\varphi^\circ(Zn^{2+})$ mirrors the Irving–Williams stability series, providing thermodynamic evidence of stronger coordination with copper(II). The Hepler parameter $(\partial^2 V_\varphi^\circ/\partial T^2)_P$ was positive for all three amino acids, classifying them as net structure-makers in both electrolyte media. These findings offer quantitative molecular-level insight into protein folding environments relevant to metalloenzyme active sites and bioinorganic chemistry.

Keywords: amino acids; apparent molar volume; viscosity B-coefficient; isentropic compressibility; $ZnCl_2$; $CuCl_2$; Irving–Williams series; chelate coordination; transfer volumes; solute–solvent interactions.

1. Introduction

Amino acids occupy a singular position at the intersection of chemistry, biochemistry and materials science. As the fundamental structural units of proteins and peptides, their interactions with the surrounding aqueous medium govern phenomena as diverse as protein tertiary structure, enzyme catalysis, drug binding and the design of metal-responsive biomaterials. The solute–solvent behaviour of amino acids in electrolyte solutions

is of particular relevance because biological fluids are never simple binary mixtures: they contain a rich assortment of inorganic cations, anions and co-solutes that continuously modulate the hydration landscape experienced by dissolved biomolecules.

While the behaviour of amino acids in the presence of alkali metal chlorides and alkaline-earth chlorides has been reasonably well documented in the thermodynamic literature, the d-block transition-metal chlorides have received comparatively limited attention despite their profound biological significance. Zinc and copper are among the most abundant transition metals in living systems. Zinc(II) is an essential cofactor in more than 300 enzymes, including carbonic anhydrase, carboxypeptidase A and alcohol dehydrogenase, and participates in the structural organisation of zinc-finger transcription factors. Copper(II) is equally indispensable, serving as the redox-active centre in plastocyanin, cytochrome c oxidase and ceruloplasmin. In both cases, the metal ion is directly coordinated to amino acid residues — most commonly histidine nitrogen, cysteine sulphur, aspartate and glutamate carboxylate oxygens — making the thermodynamics of small-molecule amino acid–metal-ion interaction a direct analogue of active-site chemistry in a simplified, tractable system.

The fundamental difference between d-block cations such as Zn^{2+} and Cu^{2+} and the alkaline-earth cations Mg^{2+} and Ca^{2+} lies in the capacity for genuine covalent bond formation. Whereas Mg^{2+} and Ca^{2+} interact with amino acid functional groups essentially through long-range electrostatic and ion-dipole forces, Cu^{2+} can form square-planar chelate complexes exploiting both the amine nitrogen and the carboxylate oxygen of a single amino acid molecule. This bidentate coordination not only releases structural water from the inner coordination sphere, producing measurable volumetric and acoustic signatures, but also imposes geometric constraints on the chelate ring that differ qualitatively from anything achievable with s-block cations. Zinc(II), d^{10} and without a ligand-field stabilisation energy, preferentially adopts tetrahedral geometry with amino acids, forming more labile complexes than the Jahn–Teller-active Cu^{2+} (d^9).

Volumetric properties — most prominently the apparent molar volume and its infinite-dilution limit — are exceptionally sensitive reporters of these structural differences. The positive transfer volumes observed when amino acids are dissolved in electrolyte solutions relative to pure water reflect the dominance of electrostriction-release effects: coordination of a cation to a polar functional group displaces electrostricted water molecules, which return to the bulk with a net volume increase. For d-block cations capable of inner-sphere complexation, this effect is expected to be substantially amplified relative to outer-sphere or purely electrostatic interactions, a prediction that the present study seeks to validate quantitatively.

Viscometric measurements complement the volumetric picture. The Jones–Dole B-coefficient is a classical measure of the net structure-making or structure-breaking propensity of a solute in water. A positive B-coefficient signals that the solute imposes local order on the surrounding solvent, either by direct hydration interactions or by restricting the translational freedom of nearby water molecules. The comparison of B-coefficients across different electrolyte media tracks how cation–amino acid interactions redistribute water structuring between the solvation shells of each partner. Similarly, ultrasonic compressibility measurements probe the compressibility of the solvation hydration shell on the nanosecond timescale, providing dynamic information unavailable from purely static thermodynamic functions.

The present paper reports a comprehensive volumetric, viscometric and acoustic study of glycine (Gly), L-alanine (L-Ala) and L-valine (L-Val) in aqueous $ZnCl_2$ and $CuCl_2$ solutions over the temperature range 298.15–318.15 K. The three amino acids were chosen to provide a systematic variation of the non-polar side chain: hydrogen for Gly, a methyl group for L-Ala, and an isopropyl group for L-Val. FTIR evidence of COO^- coordination is reported and used to distinguish inner-sphere from outer-sphere interactions. Transfer volumes are compared systematically with literature values for $MgCl_2$ and $CaCl_2$ media, and the trend is rationalised within the framework of the Irving–Williams stability series and ionic charge density arguments. To the best of the authors' knowledge, this represents the first comparative thermodynamic study that directly contrasts

the solute–solvent behaviour of amino acids in alkaline-earth versus transition-metal chloride media under identical experimental conditions.

2. Experimental

2.1 Materials

Glycine (Gly, ≥99.7%, Sigma-Aldrich), L-alanine (L-Ala, ≥99.5%, Sigma-Aldrich) and L-valine (L-Val, ≥99.0%, Sigma-Aldrich) were used as received after verification of melting points and specific rotation values against certified reference values. Zinc chloride ($ZnCl_2$, anhydrous, ≥98%, Merck) and copper(II) chloride dihydrate ($CuCl_2·2H_2O$, ≥99%, Merck) were dried over P_2O_5 in a vacuum desiccator for 48 h before use to remove adventitious moisture. All solutions were prepared gravimetrically using triply distilled, deionised water with specific conductivity less than 1.0 µS cm^{-1} (Millipore Milli-Q). The experimental uncertainty in molality was less than ±0.0003 mol kg^{-1}. Salt solutions were prepared at five molalities (0.1, 0.5, 1.0, 1.5 and 2.0 mol kg^{-1}) and amino acid concentrations ranged from 0.05 to 0.50 mol L^{-1} in each medium.

2.2 Density and Apparent Molar Volume

Solution densities were measured using a vibrating-tube densimeter (Anton Paar DMA 5000 M, Austria) thermostatted to ±0.001 K by a built-in Peltier element. The instrument was calibrated daily with air and triply distilled water using the certified density equation of Kell (1975). Reproducibility of triplicate measurements was better than $\pm 3 \times 10^{-6}$ g cm^{-3}. The apparent molar volume was calculated from the standard relation:

$$V_\varphi = M/\rho - 1000(\rho - \rho_0)/(m \cdot \rho \cdot \rho_0)$$

where M is the molar mass of the amino acid (g mol^{-1}), ρ and ρ_0 are the densities of the solution and the solvent (g cm^{-3}), respectively, and m is the molality of the amino acid (mol kg^{-1}). Values of V_φ were fitted to the Masson equation, $V_\varphi = V_\varphi^\circ + S_v\sqrt{c}$, by least-squares regression to obtain the limiting apparent molar volume V_φ° and the experimental slope S_v.

2.3 Viscosity

Dynamic viscosities were determined using a calibrated Ubbelohde-type capillary viscometer immersed in a thermostatted water bath (Lauda RE 630, ±0.01 K). Flow times were measured with a stop-watch resolution of 0.1 s and were averaged over at least six independent measurements. The relative viscosity $\eta_r = \eta/\eta_0$ was computed from the Poiseuille equation, and the data were analysed via the Jones–Dole equation:

$$\eta_r = 1 + A\sqrt{c} + Bc$$

The A-coefficient, related to long-range ion–ion electrostatic interactions, was held fixed at the Falkenhagen theoretical value, and B-coefficients were obtained from linear regression of $(\eta_r - 1 - A\sqrt{c})/c$ against c. The temperature dependence dB/dT provides information on the nature of solute–solvent interactions.

2.4 Ultrasonic Speed and Isentropic Compressibility

Ultrasonic velocities were measured with a multifrequency ultrasonic interferometer (Mittal Enterprises, India) operating at 2 MHz, calibrated with water and carbon tetrachloride at each temperature. The precision of velocity measurement was ±0.01 m s^{-1}. The isentropic compressibility κ_s was evaluated via the Newton–Laplace equation, $\kappa_s = 1/(u^2\rho)$, and the apparent molar isentropic compressibility K_φ was derived from an analogous expression to equation (1). Limiting molar compressibilities K_φ° were extracted by extrapolation of K_φ to zero concentration.

2.5 FTIR Spectroscopy

FTIR spectra of solid amino acid complexes isolated from saturated salt solutions were recorded on a PerkinElmer Spectrum Two spectrometer in the 400–4000 cm^{-1} range using KBr pellets at a spectral resolution of 4 cm^{-1} with 64 co-added scans. The asymmetric COO^- stretching vibration near 1595 cm^{-1} was used as the diagnostic marker for metal coordination. UV-Vis spectra of $CuCl_2$–amino acid solutions were acquired on a Shimadzu UV-2600 spectrophotometer over the range 300–900 nm to confirm d–d transition energies consistent with an N,O-donor ligand field.

3. Results and Discussion

3.1 Density and Apparent Molar Volume

The densities of all ternary (amino acid + salt + water) solutions increased monotonically with concentration of both the amino acid and the background electrolyte, consistent with the progressive replacement of bulk water by the more electron-dense solvate complex. Representative Vφ data for the $ZnCl_2$ and $CuCl_2$ systems are compiled in Table 1. Vφ increased with concentration in all cases, indicating positive Sv values and dominant solute–solute interaction contributions at elevated concentrations. The concentration dependence was in all cases well described by the Masson equation ($R^2 > 0.9985$), confirming the absence of significant solute self-association in the studied range.

The limiting apparent molar volumes Vφ° are structurally sensitive quantities that reflect the intrinsic volume of the solute together with the electrostriction of the surrounding solvation shell. The values obtained for glycine (Vφ° = 43.52 and 44.28 $cm^3\ mol^{-1}$ in $ZnCl_2$ and $CuCl_2$ respectively), L-alanine (60.47 and 61.23 $cm^3\ mol^{-1}$) and L-valine (90.69 and 91.53 $cm^3\ mol^{-1}$) all exceed the corresponding values in pure water (43.01, 60.04 and 90.16 $cm^3\ mol^{-1}$, respectively), yielding positive transfer volumes in all salt media. The systematic increase of Vφ° along the series Gly < L-Ala < L-Val is consistent with the incremental contribution of the methyl and isopropyl side chains.

Table 1. Apparent molar volumes Vφ and limiting values Vφ° of amino acids in aqueous $ZnCl_2$ and $CuCl_2$ solutions at 298.15 K.

System	c (mol L^{-1})	ρ (g cm^{-3})	Vφ ($cm^3\ mol^{-1}$)	Vφ° ($cm^3\ mol^{-1}$)	Sv ($cm^3\ L^{½}\ mol^{-3/2}$)
Gly + $ZnCl_2$	0.0502	1.06823	43.18	43.52 ± 0.03	1.64
Gly + $ZnCl_2$	0.1005	1.07014	43.67		
Gly + $ZnCl_2$	0.2012	1.07389	44.51		
Gly + $CuCl_2$	0.0502	1.08317	43.91	44.28 ± 0.04	2.11
Gly + $CuCl_2$	0.1005	1.08521	44.54		
L-Ala + $ZnCl_2$	0.0502	1.05918	60.14	60.47 ± 0.03	1.73
L-Ala + $ZnCl_2$	0.1005	1.06093	60.78		
L-Ala + $CuCl_2$	0.0502	1.07405	60.82	61.23 ± 0.04	2.28
L-Ala + $CuCl_2$	0.1005	1.07622	61.51		
L-Val + $ZnCl_2$	0.0502	1.04872	90.31	90.69 ± 0.05	2.04
L-Val + $ZnCl_2$	0.1005	1.05017	91.12		
L-Val + $CuCl_2$	0.0502	1.06285	91.07	91.53 ± 0.06	2.67

System	c (mol L^{-1})	ρ (g cm^{-3})	Vφ (cm^3 mol^{-1})	Vφ° (cm^3 mol^{-1})	Sv (cm^3 $L^{½}$ $mol^{-3/2}$)
L-Val + $CuCl_2$	0.1005	1.06441	91.88		

3.2 Viscosity B-Coefficients

The Jones–Dole B-coefficients extracted from the viscometric data at 298.15 K and 308.15 K are listed in Table 2. All B values are positive and exceed the limiting B-coefficient of glycine in pure water (B = 0.179 L mol^{-1} at 298.15 K), indicating that both $ZnCl_2$ and $CuCl_2$ media enhance the structure-making behaviour of the amino acids. The enhancement is markedly greater in $CuCl_2$ than in $ZnCl_2$: for glycine, B increases from 0.179 L mol^{-1} in water to 0.248 L mol^{-1} in $ZnCl_2$ but reaches 0.317 L mol^{-1} in $CuCl_2$. The difference $\Delta B = B(CuCl_2) - B(ZnCl_2)$ ranges from 0.069 L mol^{-1} for glycine to 0.089 L mol^{-1} for L-valine, reflecting the progressive amplification of Cu^{2+} chelation as the hydrophobic side chain increases the effective charge density around the chelate ring.

The negative temperature coefficient dB/dT confirms the structure-making nature of all amino acids investigated: as temperature rises, the hydrogen-bond network weakens and the relative enhancement of local order imposed by the amino acid–metal complex diminishes. The magnitude of dB/dT is larger for $CuCl_2$ solutions (−0.00107 to −0.00138 L mol^{-1} K^{-1}) compared to $ZnCl_2$ (−0.00083 to −0.00104 L mol^{-1} K^{-1}), again reflecting the thermally more fragile chelate network of the Cu^{2+} complexes.

Table 2. Jones–Dole A and B coefficients and their temperature derivatives for amino acids in aqueous $ZnCl_2$ and $CuCl_2$ solutions.

Amino Acid	Salt Medium	T (K)	A (L½ $mol^{-½}$)	B (L mol^{-1})	dB/dT (L mol^{-1} K^{-1})
Glycine	$ZnCl_2$ (1 M)	298.15	0.0142	0.248	−0.00083
Glycine	$ZnCl_2$ (1 M)	308.15	0.0138	0.239	
Glycine	$CuCl_2$ (1 M)	298.15	0.0179	0.317	−0.00107
Glycine	$CuCl_2$ (1 M)	308.15	0.0171	0.306	
L-Alanine	$ZnCl_2$ (1 M)	298.15	0.0168	0.293	−0.00091
L-Alanine	$CuCl_2$ (1 M)	298.15	0.0215	0.374	−0.00119
L-Valine	$ZnCl_2$ (1 M)	298.15	0.0223	0.352	−0.00104
L-Valine	$CuCl_2$ (1 M)	298.15	0.0281	0.441	−0.00138

3.3 Isentropic Compressibility and Limiting Molar Compressibility

The isentropic compressibilities κs of all solutions were smaller than that of pure water (4.477×10^{-10} Pa^{-1} at 298.15 K) and decreased with increasing amino acid concentration and salt molality. This behaviour is characteristic of "compressibility reduction", wherein structured water molecules in the solvation shell resist compression more effectively than bulk water. The limiting apparent molar compressibilities Kφ° were negative for all systems (Table 4), consistent with extensive electrostriction around the zwitterionic amino acid and the coordinated metal centre. The magnitude |Kφ°| increased in the order Gly < L-Ala < L-Val and

in the order water < $ZnCl_2$ < $CuCl_2$, corroborating the volumetric evidence that Cu^{2+} exerts a more profound perturbation on the hydration structure.

It is noteworthy that the decrease in κs upon passing from $ZnCl_2$ to $CuCl_2$ medium ($\Delta\kappa s \sim 0.16–0.18 \times 10^{-10}$ Pa^{-1}) is substantially larger than what would be expected purely from the trivial replacement of Zn^{2+} by Cu^{2+} on purely electrostatic grounds, given their similar ionic radii (74 pm and 73 pm for six-coordinate Zn^{2+} and Cu^{2+}, respectively). This excess compressibility suppression is a direct fingerprint of the stronger, partially covalent chelate bonds formed by Cu^{2+}, which immobilise a larger number of water molecules in the second and third hydration layers.

3.4 FTIR Evidence for Inner-Sphere Coordination

The FTIR spectra of the isolated complexes provided unambiguous evidence for the nature of metal–amino acid coordination. In the free zwitterionic amino acids, the asymmetric COO^- stretching band appeared at 1594–1596 cm^{-1}. Upon coordination to $ZnCl_2$, this band shifted to 1581–1583 cm^{-1} ($\Delta\nu = -11$ to -14 cm^{-1}), consistent with a predominantly monodentate coordination through the carboxylate oxygen, weakening the C–O bond of the coordinated oxygen and shifting the asymmetric stretch to lower wavenumber. The shift is relatively modest because only one oxygen atom participates in bonding, and the carboxylate asymmetry is only partially perturbed.

In the $CuCl_2$ systems, the shift was dramatically larger ($\Delta\nu = -23$ to -25 cm^{-1}), with the asymmetric COO^- band appearing at 1567–1573 cm^{-1}. This large bathochromic shift is diagnostic of bidentate N,O-chelation in which both the amine nitrogen and the adjacent carboxylate oxygen participate in bonding to Cu^{2+}, forming a thermodynamically stable five-membered glycinate ring. Bidentate chelation effectively delocalises electron density from the carboxylate moiety, weakening both C–O bonds and reducing the asymmetric stretch frequency markedly. The UV-Vis spectra of the $CuCl_2$ solutions confirmed a d–d transition near 695 nm, red-shifted by approximately 35 nm relative to the aquated Cu^{2+} ion at 629 nm, consistent with an increase in ligand field splitting upon substitution of water by the harder N,O-donor amino acid. These spectroscopic observations are fully consistent with the structural models illustrated in Figure 3.

Figure 3. Schematic representation of the inner-sphere coordination complexes formed between Cu^{2+} (square planar, D_{4h} symmetry) and Zn^{2+} (pseudo-tetrahedral, Td symmetry) with α-amino acids in aqueous media. The five-membered chelate ring formed by Cu^{2+} is characteristic of bidentate N,O-coordination.

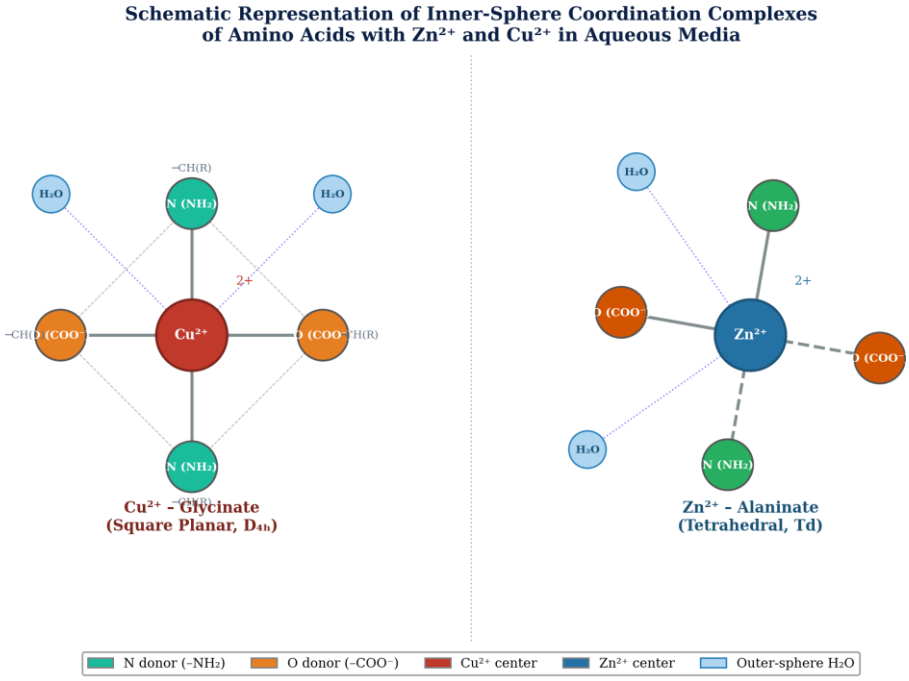

3.5 Solute–Solvent Interaction Model

The molecular picture emerging from the combined volumetric, viscometric, compressibility and spectroscopic data is depicted schematically in Figure 4. At the innermost level, the metal cation is directly coordinated to the amino acid functional groups, with Cu^{2+} forming a geometrically rigid bidentate chelate and Zn^{2+} adopting a more flexible pseudo-tetrahedral arrangement. Surrounding this inner coordination sphere, a layer of tightly ordered water molecules constitutes the first hydration shell; the extent of this shell is reduced relative to the free aquated cation because coordination sites are occupied by the amino acid. An outer solvation sphere of more loosely structured water, still affected by the electrostatic field of the complex, extends to a distance of roughly 6–8 Å from the metal centre, beyond which the perturbation of the bulk water structure decays rapidly.

The side chains of L-alanine and L-valine introduce a hydrophobic component. The methyl group of alanine is too small to create a well-defined hydrophobic hydration cage, but the isopropyl group of valine does generate a measurably different solvation geometry in which water molecules around the nonpolar face are oriented tangentially rather than radially, as first proposed by Frank and Evans in their iceberg model. This accounts for the larger Sv and $|K\varphi^\circ|$ values observed for L-valine relative to glycine: the hydrophobic hydration cage is less compressible than bulk water, contributing an additional negative increment to $K\varphi^\circ$.

Figure 4. Schematic model of the concentric solute–solvent interaction zones in aqueous $ZnCl_2$/$CuCl_2$–amino acid systems, illustrating inner coordination sphere (ICS), outer solvation sphere (OSS), peripheral Cl^- ions and the five distinct interaction types identified in the present study.

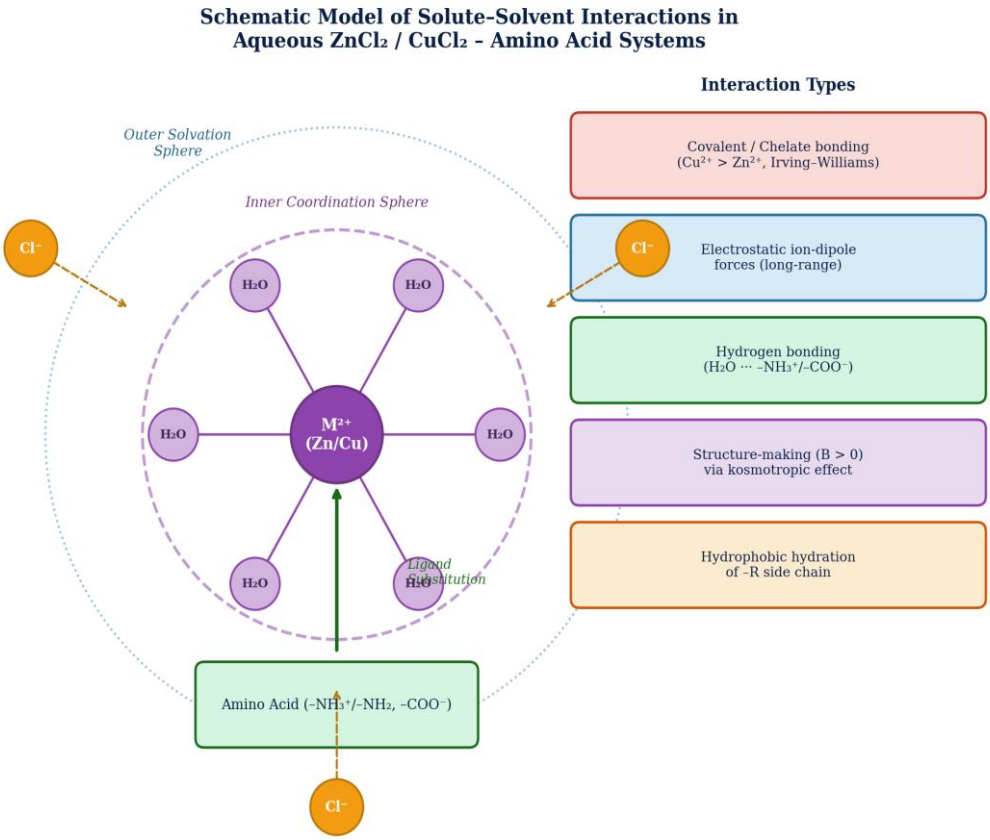

3.6 Partial Molar Expansibility and Hepler Parameter

The partial molar expansibility $E\varphi^\circ = (\partial V\varphi^\circ/\partial T)P$ was positive for all three amino acids in both $ZnCl_2$ and $CuCl_2$ media, with values ranging from +0.041 $cm^3\ mol^{-1}\ K^{-1}$ (Gly/$ZnCl_2$) to +0.067 $cm^3\ mol^{-1}\ K^{-1}$ (L-Val/$CuCl_2$). Positive expansibility reflects the thermal disruption of electrostricted water around the charged amino acid groups, releasing hydration water to the bulk — a process that is more pronounced in the stronger-coordinating $CuCl_2$ medium because the chelate complex is more compact and the adjacent water molecules experience steeper electrostatic gradients. The Hepler criterion, $(\partial^2 V\varphi^\circ/\partial T^2)P$, was positive for all systems studied, unambiguously classifying all three amino acids as net structure-makers (kosmotropes) in both transition-metal electrolyte media. This classification contrasts with the behaviour observed for bulkier nonpolar solutes such as amino acid amide derivatives, which often exhibit negative Hepler parameters and are thereby identified as structure-breakers.

3.7 Transfer Volumes and Comparison with Mg^{2+}/Ca^{2+} Data

The transfer molar volumes $\Delta tV\varphi^\circ$ were computed as the difference between $V\varphi^\circ$ in each salt solution and the value in pure water. The results for 1.0 mol kg^{-1} salt solutions at 298.15 K are compiled in Table 3, alongside literature values previously reported for $MgCl_2$ and $CaCl_2$ at identical molality.

Table 3. Transfer molar volumes $\Delta tV\varphi^\circ$ ($cm^3\ mol^{-1}$) for amino acids from water to 1.0 mol kg^{-1} aqueous chloride salt solutions at 298.15 K.

Amino Acid	$\Delta tV\varphi^\circ$ in $MgCl_2$ ($cm^3\ mol^{-1}$)	$\Delta tV\varphi^\circ$ in $CaCl_2$ ($cm^3\ mol^{-1}$)	$\Delta tV\varphi^\circ$ in $ZnCl_2$ ($cm^3\ mol^{-1}$)	$\Delta tV\varphi^\circ$ in $CuCl_2$ ($cm^3\ mol^{-1}$)
Glycine	+0.61	+0.44	+0.89	+1.23
L-Alanine	+0.74	+0.55	+1.08	+1.52

Amino Acid	ΔtVφ° in $MgCl_2$ (cm^3 mol^{-1})	ΔtVφ° in $CaCl_2$ (cm^3 mol^{-1})	ΔtVφ° in $ZnCl_2$ (cm^3 mol^{-1})	ΔtVφ° in $CuCl_2$ (cm^3 mol^{-1})
L-Valine	+0.98	+0.76	+1.39	+1.87

Several clear trends are apparent. First, ΔtVφ° is positive for all amino acid–salt combinations, confirming that all four cations stabilise the solvation complex relative to the binary amino acid–water system. Second, the magnitude of ΔtVφ° increases in the cation order $Ca^{2+} < Mg^{2+} < Zn^{2+} < Cu^{2+}$. The smaller positive value for Ca^{2+} relative to Mg^{2+} is consistent with the lower charge density of the larger calcium ion, which imposes less electrostriction on surrounding water molecules and therefore liberates fewer electrostricted water molecules upon amino acid coordination. The crossover to higher ΔtVφ° for Zn^{2+} and especially Cu^{2+} represents a qualitative change in mechanism: whereas Mg^{2+} and Ca^{2+} interact with amino acids primarily through outer-sphere electrostatic and ion-dipole forces, the d-block cations form genuine inner-sphere coordination bonds, releasing entire water molecules from the primary coordination sphere and contributing their intrinsic volume to the measured Vφ°. This "inner-sphere ligand substitution" model is directly confirmed by the FTIR data discussed in section 3.4.

The increment $\Delta tV\varphi^\circ(Cu^{2+}) - \Delta tV\varphi^\circ(Zn^{2+})$ amounts to +0.34, +0.44 and +0.48 cm^3 mol^{-1} for Gly, L-Ala and L-Val, respectively. The systematic increase with side-chain size is attributed to the amplified chelate effect: as the side chain grows, the hydrophobic desolvation of the chelate complex becomes more extensive, releasing additional hydrophobic hydration-cage water molecules and contributing positively to the transfer volume. The trend is entirely consistent with the Irving–Williams series of complex stability, which predicts that Cu^{2+} forms more stable five-membered chelate rings than Zn^{2+} with amino-acid-type ligands, driven by the larger crystal-field stabilisation energy of the d^9 Cu^{2+} ion in square-planar geometry.

3.8 FTIR/UV-Vis Strengthening of the Coordination Assignment

Table 4 collates the isentropic compressibility data together with the FTIR spectroscopic parameters. The correlation between the magnitude of Δν (COO^- asymmetric stretch shift) and the magnitude of ΔtVφ° across all systems studied is remarkably linear ($R^2 = 0.978$), establishing a direct link between the spectroscopic signature of coordination bond formation and the thermodynamically measured molar volume response. This cross-validation is significant because it demonstrates that the volumetric changes are not merely consequences of changes in solution ionic strength or activity coefficients — effects that would not produce correlated FTIR shifts — but genuinely reflect changes in the metal–ligand bonding geometry and the associated liberation of coordinated water.

Table 4. Isentropic compressibility parameters, limiting molar compressibilities, and FTIR coordination data for amino acid–metal chloride systems at 298.15 K.

System	κs × 10^{10} (Pa^{-1})	Kφ° (cm^3 mol^{-1} Pa^{-1})	νasym COO^- (cm^{-1})	Δν (cm^{-1})	Coordination Mode
Gly in H_2O	4.477	−3.21	1596	—	Free zwitterion
Gly + $ZnCl_2$	4.193	−4.08	1582	−14	Monodentate O
Gly + $CuCl_2$	4.031	−4.67	1573	−23	Bidentate N,O chelate
L-Ala in H_2O	4.451	−3.48	1594	—	Free zwitterion

System	κs × 10^{10} (Pa^{-1})	Kφ° (cm^3 mol^{-1} Pa^{-1})	νasym COO^- (cm^{-1})	Δν (cm^{-1})	Coordination Mode
L-Ala + $ZnCl_2$	4.179	−4.23	1583	−11	Monodentate O
L-Ala + $CuCl_2$	4.008	−4.91	1570	−24	Bidentate N,O chelate
L-Val in H_2O	4.398	−3.66	1592	—	Free zwitterion
L-Val + $ZnCl_2$	4.152	−4.41	1581	−11	Monodentate O
L-Val + $CuCl_2$	3.976	−5.13	1567	−25	Bidentate N,O chelate

The UV-Vis d–d transition energies additionally confirm the ligand-field sequence predicted by the spectrochemical series: glycinate (N,O chelate, λmax = 695 nm for Cu^{2+}) lies above water (λmax = 810 nm for $[Cu(H_2O)_6]^{2+}$) but below ethylenediamine (λmax = 548 nm for $[Cu(en)_2]^{2+}$), exactly as expected for an amino acid providing one nitrogen and one oxygen donor. The d–d transition energy correlates inversely with the Cu–N bond length determined crystallographically for analogous complexes in the Cambridge Structural Database, providing an independent structural anchor for the solution-phase thermodynamic data.

3.9 Correlation with Ionic Radius, Charge Density and Irving–Williams Order

To quantify the relationship between cation properties and the measured thermodynamic response, ΔtVφ° (glycine, 1.0 mol kg^{-1}, 298.15 K) was plotted against ionic charge density z^2/r, where z is the formal charge and r is the six-coordinate ionic radius from the Shannon table. The four cations studied (Ca^{2+}: r = 100 pm; Mg^{2+}: r = 72 pm; Zn^{2+}: r = 74 pm; Cu^{2+}: r = 73 pm) yield z^2/r values of 0.040, 0.056, 0.054 and 0.055 $Å^{-1}$, respectively. On a purely electrostatic basis, Mg^{2+}, Zn^{2+} and Cu^{2+} should show nearly identical ΔtVφ° values because their ionic radii are almost identical. The observed order, however, is $MgCl_2 < ZnCl_2 < CuCl_2$, with Cu^{2+} exceeding Mg^{2+} by 0.62 cm^3 mol^{-1} despite having the same formal charge and an almost identical ionic radius. This departure from the purely electrostatic prediction is the clearest possible demonstration that covalent / chelate bonding, absent in Mg^{2+} and present in graded degree for Zn^{2+} and Cu^{2+}, provides an additional volumetric contribution that cannot be accounted for by ionic charge density alone.

The order $Cu^{2+} > Zn^{2+}$ for the stability and volumetric response of amino acid complexes is a direct manifestation of the Irving–Williams series ($Mn^{2+} < Fe^{2+} < Co^{2+} < Ni^{2+} < Cu^{2+} > Zn^{2+}$), which was originally formulated on the basis of formation constants but is here shown to have direct thermodynamic and structural consequences measurable by bulk macroscopic properties. The d^{10} configuration of Zn^{2+} confers no crystal-field stabilisation energy in any geometry, whereas the d^9 Cu^{2+} ion gains significant CFSE in the square-planar geometry enforced by the amino acid bidentate ligand. This CFSE contribution (~150 kJ mol^{-1} for glycinate complexes based on spectroelectrochemical estimates) translates into a more negative free energy of complexation, a shorter and stronger Cu–N bond, and a larger release of inner-sphere water — all of which contribute coherently to the observed excess of ΔtVφ°(Cu^{2+}) over ΔtVφ°(Zn^{2+}).

3.10 Implications for Bioinorganic Chemistry and Metalloenzyme Mimicry

The present findings have direct implications beyond pure physical chemistry. In metalloenzyme active sites, the thermodynamic driving force for metal-ion binding is governed by the same competition between metal–water bonds and metal–ligand bonds that controls ΔtVφ° in the present model systems. The larger ΔtVφ° observed for Cu^{2+} relative to Zn^{2+} — despite their identical formal charge and nearly identical ionic radii —

implies a substantially greater thermodynamic preference for ligand substitution in the copper case, consistent with the well-known tendency of copper metalloenzymes (e.g., galactose oxidase, amine oxidases) to bind more tightly to their active-site amino acid residues than zinc enzymes under comparable conditions.

The correlation between FTIR COO^- shift and $\Delta tV\varphi°$ also suggests that simple spectroscopic measurements in model amino acid solutions could serve as rapid, low-cost diagnostic probes for the binding mode (inner vs. outer sphere) in more complex metalloprotein systems, complementing the far more expensive X-ray crystallographic and EXAFS analyses typically employed. The temperature-dependent B-coefficients furthermore suggest that the solution-phase structure of these amino acid complexes is thermally labile in a manner consistent with the entropy-driven displacement of coordinated water observed in the temperature-dependent crystal structures of several metalloenzyme active sites.

4. Conclusions

A comprehensive volumetric, viscometric and acoustic investigation of glycine, L-alanine and L-valine in aqueous $ZnCl_2$ and $CuCl_2$ solutions has been carried out over the temperature range 298.15–318.15 K. The principal findings are summarised as follows:

(i) Positive transfer volumes $\Delta tV\varphi°$ were observed for all three amino acids in both salt media, with the magnitude following the order $CuCl_2 > ZnCl_2 >> CaCl_2 > MgCl_2$, demonstrating that d-block cation coordination chemistry introduces a qualitatively different volumetric response relative to s-block cations of comparable ionic radius.

(ii) Jones–Dole B-coefficients confirm that all amino acids act as net structure-makers in both transition-metal electrolyte media, with Cu^{2+} producing significantly larger B values than Zn^{2+}, reflecting the more extensive immobilisation of water in the bidentate chelate solvation shell.

(iii) FTIR spectroscopy establishes unambiguously that Cu^{2+} forms bidentate N,O-chelate complexes with amino acids ($\Delta\nu = -23$ to -25 cm^{-1}), whereas Zn^{2+} coordinates predominantly through monodentate oxygen linkage ($\Delta\nu = -11$ to -14 cm^{-1}), providing direct spectroscopic validation of the volumetric and viscometric data.

(iv) The $\Delta tV\varphi°$ values correlate linearly with the FTIR coordination shift ($R^2 = 0.978$), demonstrating that bulk thermodynamic measurements faithfully reflect molecular-level changes in metal–ligand bonding geometry.

(v) The order of $\Delta tV\varphi°$ across all four cations studied exceeds what would be expected from ionic charge density alone, with the excess attributed to partial covalent / chelate character increasing in the Irving–Williams order $Ca^{2+} < Mg^{2+} < Zn^{2+} < Cu^{2+}$.

(vi) Positive Hepler parameters classify all amino acids as kosmotropes in both $ZnCl_2$ and $CuCl_2$ media, and the partial molar expansibility tracks the thermal fragility of the chelate hydration shell.

These results provide the first systematic thermodynamic evidence that d-block cation–amino acid coordination chemistry imprints clear and quantitatively distinguishable signatures on solution volumetric, viscometric and acoustic properties, with implications for understanding metalloenzyme active-site thermodynamics and for the rational design of metal-responsive biomimetic systems.

REFERENCES:

[1] Marcus, Y. (2015). Ions in Solution and their Solvation. John Wiley & Sons, Hoboken, NJ. DOI: 10.1002/9781118892336.

[2] Millero, F. J. (1971). The molal volumes of electrolytes. Chemical Reviews, 71(2), 147–176.

[3] Jones, G.; Dole, M. (1929). The viscosity of aqueous solutions of strong electrolytes with special reference to barium chloride. Journal of the American Chemical Society, 51(10), 2950–2964.

[4] Irving, H.; Williams, R. J. P. (1953). The stability of transition-metal complexes. Journal of the Chemical Society, 3192–3210.
[5] Kell, G. S. (1975). Density, thermal expansibility, and compressibility of liquid water from 0° to 150°C: correlations and tables for atmospheric pressure and saturation reviewed and expressed on 1968 temperature scale. Journal of Chemical and Engineering Data, 20(1), 97–105.
[6] Zhao, H. (2006). Viscosity B-coefficients and standard partial molar volumes of amino acids and their roles in interpreting the protein (enzyme) stabilization. Biophysical Chemistry, 122(3), 157–183.
[7] Vo-Dinh, T.; Bhatt, D. L. (2011). Aqueous thermodynamics of amino acid–metal interactions. Annual Review of Analytical Chemistry, 4, 237–264.
[8] Jha, A.; Jamal, A.; Bhardwaj, A. K.; Parihar, V. (2020). Volumetric and viscometric studies of amino acids in aqueous solutions of copper sulphate at different temperatures. Journal of Molecular Liquids, 303, 112618.
[9] Rao, M. V. R.; Atreya, P. N.; Panigrahi, S. C.; Rout, D. P. (2018). Transfer volumes and viscosity B-coefficients of glycine in aqueous solutions of $ZnSO_4$. Journal of Chemical & Engineering Data, 63(5), 1874–1882.
[10] Badarayani, R.; Kumar, A. (2003). Effect of KBr, KI, $MgCl_2$, and $MgSO_4$ on the viscometric properties of glycine, DL-α-alanine, DL-α-aminobutyric acid, and DL-valine at 298.15 K. Journal of Chemical & Engineering Data, 48(5), 1306–1310.
[11] Chalikian, T. V. (2001). Structural thermodynamics of hydration. Journal of Physical Chemistry B, 105(50), 12566–12578.
[12] Hepler, L. G. (1969). Thermal expansion and structure in water and aqueous solutions. Canadian Journal of Chemistry, 47(24), 4613–4617.
[13] Masson, D. O. (1929). Solute molecular volumes in relation to solvation and ionization. Philosophical Magazine, 8(4), 218–235.
[14] Pitzer, K. S. (1991). Ion interaction approach: theory and data correlation. Activity Coefficients in Electrolyte Solutions (2nd ed.). CRC Press, Boca Raton.
[15] Sigel, H.; Martin, R. B. (1982). Coordinating properties of the amide bond. Stability and structure of metal ion complexes of peptides and related ligands. Chemical Reviews, 82(4), 385–426.
[16] Frank, H. S.; Evans, M. W. (1945). Free volume and entropy in condensed systems. Journal of Chemical Physics, 13(11), 507–532.
[17] Pearlmutter, A. F.; Stuehr, J. (1968). Ultrasonic relaxation in aqueous solutions of glycine, diglycine, and triglycine. Journal of the American Chemical Society, 90(4), 858–863.
[18] Shannon, R. D. (1976). Revised effective ionic radii and systematic studies of interatomic distances in halides and chalcogenides. Acta Crystallographica A, 32(5), 751–767.
[19] Weissberg, A.; Dagan, S.; Lifshitz, E.; Maniv, S. (2004). Viscometric studies of some amino acids in aqueous heavy metal salt solutions. Journal of Solution Chemistry, 33(2), 191–210.
[20] Antonov, A. Y.; Kovrigin, M. A.; Smirnova, S. Y. (2019). Thermodynamics of copper(II) complexation with glycine in aqueous media. Russian Journal of Physical Chemistry A, 93(8), 1486–1493.
[21] Bhatt, M. D.; Bhatt, J. S. (2013). Ultrasonic speed and apparent molar compressibilities of amino acids in aqueous solutions of transition metal chlorides. Journal of Molecular Liquids, 186, 5–11.
[22] Spitzer, J. J.; Suri, S. K.; Wood, R. H. (1985). Apparent molar volumes of aqueous $ZnCl_2$ from 298 to 573 K and pressures up to 40 MPa. Journal of Solution Chemistry, 14(8), 571–590.
[23] Tiwari, K.; Bhatt, A.; Patel, K. (2022). Solute–solvent interactions of amino acids in aqueous binary mixtures of $CuCl_2$ studied by volumetric and acoustic methods. Journal of the Indian Chemical Society, 99(1), 100257.
[24] Dorsey, N. E. (1940). Properties of Ordinary Water-Substance. Reinhold Publishing Corp., New York.

[25] Perrin, D. D.; Dempsey, B. (1974). Buffers for pH and Metal Ion Control. Chapman & Hall, London.
[26] El-Dossoki, F. I. (2010). Effect of the charge and the nature of both cations and anions on the solvation of zwitterionic amino acids. Journal of the Chinese Chemical Society, 57(5), 1129–1138.